

Article

Simulation Analysis of the Effect of Slit/Slot Pintle Geometry on Atomization of Bipropellant Engine

Kun Cai ¹, Zhen Zhang ^{1,2,*} , Fengshan Wang ¹, Yu Hu ¹, Xudong Wang ¹ , Zhicheng Fang ¹, Xiaofang Mao ¹, Zhaopu Yao ¹, Yusong Yu ²  and Haiwang Li ³

¹ Beijing Institute of Control Engineering, Beijing 100190, China; caikun_0932@163.com (K.C.)

² Hydrogen Energy and Space Propulsion Laboratory (HESPL), School of Mechanical, Electronic and Control Engineering, Beijing Jiaotong University, Beijing 100044, China

³ Tianmushan Laboratory, Hangzhou 310023, China

* Correspondence: 21114129@bjtu.edu.cn; Tel.: +86-135-8167-8506

Abstract: In order to optimize the slit/slot geometry design of a bipropellant pintle injector, the impinging spray development of a pintle injector was numerically investigated. The VOF (volume of fluid) and LES (large eddy simulation) methods were employed for an analysis to capture the gas–liquid interface by means of the AMR (adaptive mesh refinement) method. In those simulation cases, different flowrates, slot numbers, pintle diameters, slot thicknesses and slot shapes were compared for an analysis. In a comparison of visualization and quantification, a high flowrate and large pintle diameter were shown to be more positive features for improving the atomization quality and mixing effect. As for the slot parameters and shape, the spray development was mainly determined by the flow proportion between the slit jet and slot jet. The simulation results indicated that dominant slot jets cause a more dispersed spatial distribution, which is more conducive to the subsequent improvement of combustion efficiency in a limited space. However, an excessive increase in the number of slot jets can weaken the overall atomization quality and mixing effect, so it is suggested to ensure a balance for geometry design optimization.



Citation: Cai, K.; Zhang, Z.; Wang, F.; Hu, Y.; Wang, X.; Fang, Z.; Mao, X.; Yao, Z.; Yu, Y.; Li, H. Simulation Analysis of the Effect of Slit/Slot Pintle Geometry on Atomization of Bipropellant Engine. *Processes* **2023**, *11*, 2471. <https://doi.org/10.3390/pr11082471>

Academic Editors: Wenjie Wang, Lijian Shi, Fangping Tang, Kan Kan and Fan Yang

Received: 24 June 2023

Revised: 31 July 2023

Accepted: 1 August 2023

Published: 17 August 2023



Copyright: © 2023 by the authors. Licensee MDPI, Basel, Switzerland. This article is an open access article distributed under the terms and conditions of the Creative Commons Attribution (CC BY) license (<https://creativecommons.org/licenses/by/4.0/>).

Keywords: bipropellant engine; pintle injector; spray atomization; slit/slot; impingement; simulation

1. Introduction

A bipropellant engine with high performance and reliability is the key for a bipropellant propulsion system of a satellite. Its injector determines the uniform mixing of propellants and liquid film cooling through efficient spray organization. Pintle injectors have been seen as great adopted schemes with a specific design structure, which can achieve better propellant mixing through the mutual impingement of axial and radial jet flows. Their combustion efficiency can reach up to 96–99% [1]. The design of a pintle injector is to inject propellants radially through a series of slots or slits and then impinge on the axial jet flow through an annular gap outside the pintle, thus forming a cross- and orthogonal impingement to atomize propellants into fine droplets [2]. The Apollo moon landing engine LMDE developed a pintle injector to achieve the maximum thrust of 46,600 N and the thrust ratio of 10:1 [3]. A pintle injector was also employed for the Chang'e-3 soft landing to achieve the maximum thrust of 7500 N and the adjustable thrust ratio of 5:1 [4,5]. However, as for an orbit control engine with a small thrust for a spacecraft of normal size, there is generally no variable thrust requirement. Compared with large-thrust engines and variable-thrust engines, a bipropellant engine is required for a normal-sized satellite's orbit control to achieve a smaller and constant thrust. Moreover, it is always expected to achieve a high specific impulse and high reliability by taking advantage of the simple structure, stable combustion and high-performance potential of the pintle injector [6]. Therefore, it requires efficient mixing and combustion of the two propellants in a limited space through a well-organized spray and atomization.

For a pintle engine, the TMR (total momentum ratio) is the most important design parameter, which is defined as the ratio of radial momentum and axial momentum [7]. Design experience shows that the optimal performance can be achieved when the TMR value is around 1. However, for the constant-thrust engine of a normal satellite, there is almost no room to adjust the TMR value within the limited range of the pressure drop. And the annular spray is generally the only option for adjusting the outer jet flow. Therefore, the geometric design of a pintle injector has an important influence on the performance of a liquid rocket engine [8]. On the one hand, it is necessary to form a large spray angle to reduce the axis velocity of the liquid flow so that propellants can achieve better combustion in the chamber. On the other hand, it is required to form a reasonable spatial distribution and mixing effect to maximize the utilization of the limited combustion chamber space. As for the pintle radial injection, we can obtain a thin liquid sheet via the slit or the jet flow through the slots. However, it is common to use the combination of the above two in order to cause deformations of the liquid spray, resulting in complex flow field structures with a better mixing effect in a three-dimensional space.

Researchers generally investigated the influence of the TMR on atomization without too much focus on the structural design of the pintle. Son et al. mainly solved the problems of the cone angle measurement, distribution measurement and numerical exploration of a pintle injector with a radial slot using a Lagrangian approach [9–11]. They discovered that the SMD value becomes lower when the radial opening distance decreases and the Weber number increases. At Minas Gerais Federal University in Brazil, various combinations were used to determine the injection patterns of radial and annular flows, and the basic spray conditions of a prototype injector for a 1 KN engine [12]. At China's National University of Defense Technology, a numerical analysis was performed to investigate the effects of pintle injector geometry on the combustion chamber's internal combustion field. Specifically, combustion characteristics based on the characteristic length, pintle opening distance and pintle length were observed [13]. In Korea, at Chungnam National University, spray patterns and combustion performance were observed for various canted slit-type pintle injectors [14–16]. Zhou conducted an experimental study on the spray characteristics of a pintle injector element, showing that the circular hole and the square hole had a larger angle than the rectangular hole at the same injection area and velocity under the large TMR condition [17]. Chen found that the spray distribution and spray development are mainly controlled by the interaction of the radial flow of the jet and the axial flow of the film, as well as to some degree by the impingement of the liquid droplets in the spray center [18]. Cheng showed that the spray pattern and breakup rely heavily on the TMR, jet Reynolds number and film Reynolds number. And the discharge coefficient of the pintle orifice reduces when the ratio of the jet diameter to film thickness increases [19].

A connected slit/slot radial jet can improve the flow instability, and it is beneficial for atomization. The slit sprays the radial jet to impinge on the axial jet and stop it from spraying out of the combustion chamber directly. The slot is designed to make the radial jet flow more unstable and change the spray angle and droplet distribution for better atomization after impingement. However, more geometry parameters, such as the slot number, pintle diameter, slot thickness and slot shape, have been less studied regarding their influence on atomization optimization. In this study, the impinging spray of an axial annular film and a radial jet flow ejected through a connected slit/slot combination is comparatively simulated. The VOF and LES methods are used in simulations by using OpenFOAM, capturing the gas–liquid interface by means of the AMR method. Therefore, the influences of different slit/slot geometries on the impinged composite spray angle, atomization quality and mixing effect are studied for design optimization.

2. Methodology

2.1. Governing Equation

The impinging spray of a pintle injector is modeled using the VOF method. The VOF model has been widely used to capture the gas–liquid interface for an injector spray

field. Because our focus is on the spray development at room temperature without heat exchange, the governing equations with the CSF (continuous surface tension force) model are presented as Equations (1) and (2) [20,21]:

$$\nabla \cdot V = 0 \quad (1)$$

$$\rho \frac{\partial V}{\partial t} + \rho \nabla \cdot (VV) = -\nabla p + \mu \nabla V + \rho g + \sigma k \nabla \varepsilon_l \quad (2)$$

where V is the fluid velocity vector, ρ is the fluid density, p is the fluid pressure, k is the surface curvature, σ is the surface tension coefficient, g is the gravity and μ is the fluid dynamic viscosity.

In the VOF model, ε_l represents the volume fraction to describe the interface between liquid and gas with a value between 0 and 1. The mixture density ρ and mixture viscosity μ are described as Equations (3) and (4) [22]:

$$\rho = \varepsilon_l \rho_l + (1 - \varepsilon_l) \rho_g \quad (3)$$

$$\mu = \varepsilon_l \mu_l + (1 - \varepsilon_l) \mu_g \quad (4)$$

where the subscript l represents liquid, and g represents gas.

2.2. Turbulence Model

The LES method is employed to solve the second-order nonlinear partial differential equations as shown in Equations (5) and (6) [23,24]. After filtration, large-scale turbulent eddies are directly calculated and small-scale turbulent eddies are solved by adding a sublattice stress term to simulate the process of vortex breaking and turbulent kinetic energy. The incompressible equations can be filtered as

$$\frac{\partial \tilde{u}_i}{\partial x_i} = 0 \quad (5)$$

$$\frac{\partial (p\tilde{u}_i)}{\partial t} + \frac{\partial (p\tilde{u}_i\tilde{u}_j)}{\partial x_j} = \frac{\partial}{\partial x_j} (\mu \frac{\partial \tilde{u}_i}{\partial x_j}) - \frac{\partial \tilde{p}}{\partial x_i} - \frac{\partial \tau_{ij}}{\partial x_j} \quad (6)$$

where the sub-grid stress tensor τ_{ij} is obtained as Equations (7) and (8) [20,25,26]:

$$\tau_{ij} = -2\nu_t \tilde{S}_{ij} + \frac{2}{3} \delta_{ij} k_{sgs} \quad (7)$$

$$\nu_t = C_v \Delta (k_{sgs})^{1/2} \quad (8)$$

where δ_{ij} is the Kronecker symbol, \tilde{S}_{ij} is the known strain tensor, ν_t is the turbulent eddy viscosity, Δ is the filter scale, and sublattice viscosity k_{sgs} is calculated by different methods in the LES method. The k-equation model is a single-equation model based on the eddy viscosity assumption to calculate k_{sgs} from its transport equation as

$$\frac{\partial k_{sgs}}{\partial t} + \frac{\partial \tilde{u}_j k_{sgs}}{\partial x_j} = \frac{\partial}{\partial x_j} (\nu_t \frac{\partial k_{sgs}}{\partial x_j}) - \tau_{ij} \tilde{S}_{ij} - C_\varepsilon \frac{(k_{sgs})^{3/2}}{\Delta} \quad (9)$$

where C_ε and C_v are constant coefficients, which need to be assigned or dynamically obtained.

2.3. Physical Model

A whole simulation domain with a diameter of 72 mm is shown as Figure 1. The geometric model of a pintle injector is mainly composed of an inlet, a pintle injector with an axial annular nozzle and a radial slit/slot nozzle, a spray domain, chamber walls and an outlet. There are two multiphase inlets with two fixed flowrate boundaries. The MMH

(monomethyl hydrazine) fuel is sprayed from an annular gap, called an outer spray. And the NTO (nitrogen tetroxide) oxidizer is set to fill the inner volume of the pintle and then sprayed out through the radial slit/slot nozzle, called an inner spray. Those two jets impinge each other and then mix in the spray domain at a total pressure of 100 Pa. The mixed spray is developed in the limited space and impacts on the chamber wall to form a liquid film. Skip distance is defined as the distance from the axial nozzle to the propellant impingement point, which mainly regulates the size of backflows.

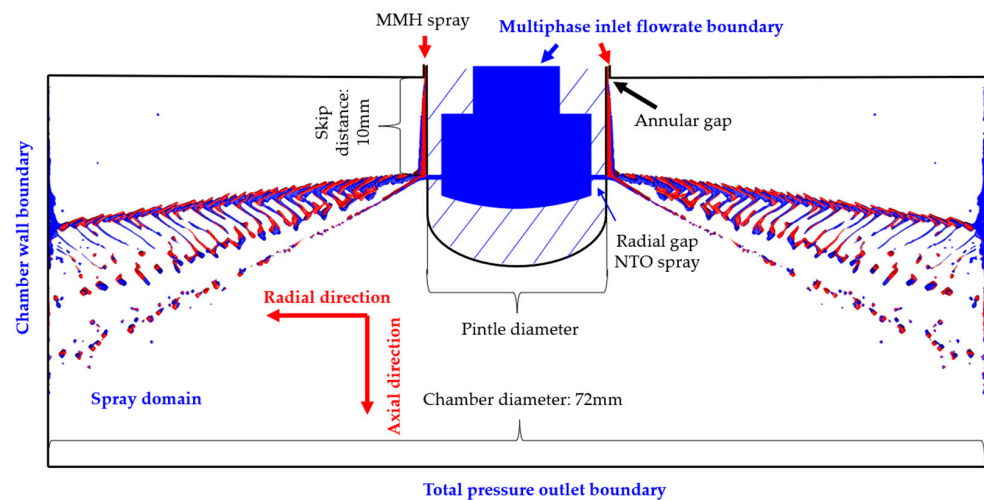


Figure 1. Schematic of the simulation domain.

In order to reduce the total number of grids in the simulation, two methods are employed in this study. The first method is that the whole simulation domain is evenly divided into an arc region, and its radian is equal to the quotient of 360° divided by the number of slots. That means each spray domain can include a single radial slit/slot nozzle with a cross-section as shown in Figure 2. The second method is to conduct the AMR method going with a liquid–gas interface gradient in OpenFOAM [27,28], for enhancing the capture capability of the liquid–gas interface.

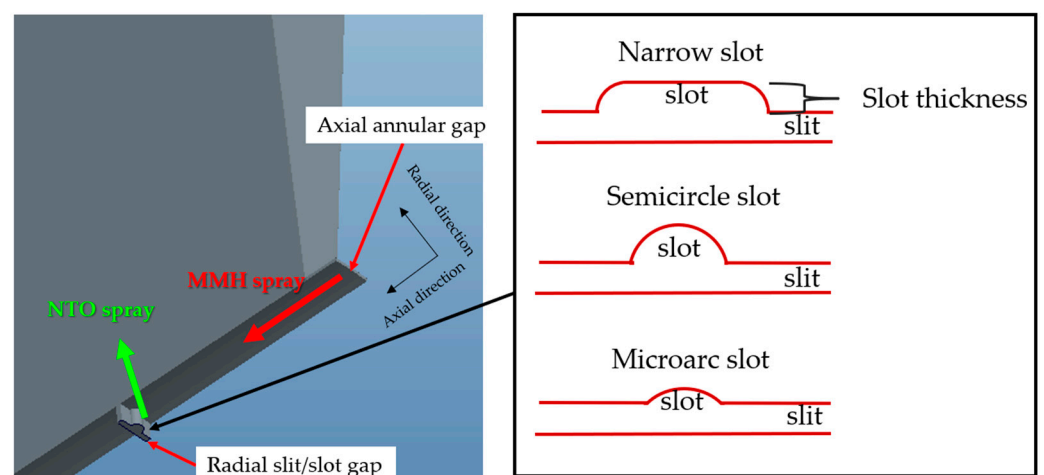


Figure 2. Combination structure with different types of slit and slot.

There are three types of a slot connected with a narrow slit, and this combination is designed to enhance radial jet instability and strengthen the droplets breakup and mixing effect after impingement. In particular, as for a narrow slot, it is composed of a rectangular slot with semicircular corners on both sides. The length of narrow slots is fixed, so the flowrate proportion of the slot and slit can be changed by adjusting the thickness of the slot

and slit, as shown in Figure 2. The mixture ratio of NTO to MMH is 1.65:1, and 25% of the MMH flow is used for cooling, so the NTO spray is absolutely in a strong position. The TMR is set to be around 2 for these two propellants impingement.

2.4. Mesh Generation and Boundary Condition

The snappyHexMesh tool is used to generate a 3D mesh in OpenFOAM, as shown in Figure 3. The initial side length of a mesh grid is 0.1 mm, so it can be decreased to 12.5 μm after three times refinements at the maximum. Additionally, those grids near a boundary area can be further refined.

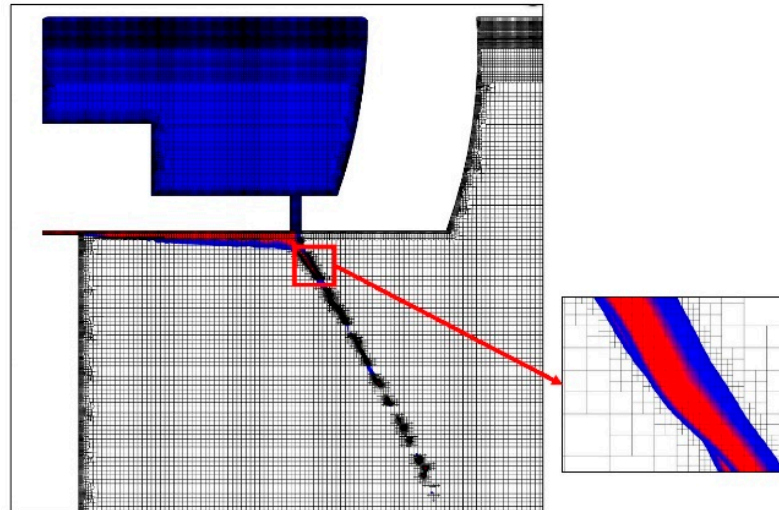


Figure 3. Adaptive mesh refinement.

The inlet boundary condition is a constant flowrate inlet. Its flowrate value is set to be the design flowrate in the arc domain. The injection pressure drop of the inner MMH nozzle is about 0.6 MPa, and that of the outer NTO nozzle is about 0.5 MPa. So, many tests were conducted to adjust the nozzle size in the modeling construction in order to keep the pressure drop almost unchanged under different conditions. The outlet boundary is the fixed total pressure of 100 Pa. In the initial condition, the MMH and the NTO are set to fill the inner flow chamber directly to the axial nozzle and the radial nozzle. That means, when the simulation starts to run, the nozzle can immediately spray two propellants out.

2.5. Postprocessing Method

The total surface area of sprayed liquid is calculated by integrating all areas of the gas–liquid interface in the spray domain. It is denoted as S_{spray} . Considering different spray conditions, the total surface area ratio R_{spray} is obtained for a fair quantitative comparison by dividing a reference area, which is the calculated area of a continuous jet flow denoted as S_{ref} , as presented in Equation (10) [29]. This S_{ref} is calculated by multiplying the gap perimeter of the nozzle by the injection velocity and then by the injection time.

$$R_{\text{spray}} = S_{\text{spray}} / S_{\text{ref}} \quad (10)$$

As mentioned, ε_l represents the volume fraction to describe gas–liquid interface. Those values between 0 and 1 can describe a critical state. In the spray domain, all regions with ε_l value of both MMH phase and NTO phase between 0 and 1 at the same time are marked. Eventually, the total surface area of these marked regions is obtained by statistics and integration, called mixed area. The mixed area is used to evaluate the mixing effect of two propellants.

2.6. Simulation Validation

As for mesh independence, three cases were solved on initial grid resolutions with 0.08 mm size, 0.1 mm size and 0.12 mm size. The composite spray angles after impingement were the same. And R_{spray} in the case of 0.12 mm mesh is slightly larger than that in cases of 0.1 mm mesh and 0.08 mm mesh by about 3%. But the difference between the latter two cases is only 0.52%. It is indicated that 0.1 mm mesh size can meet the simulation requirement.

In order to further validate the simulation method, the VOF and LES method were used to compare with a reference experimental result as shown in Figures 4 and 5 [30]. Modeling was carried out according to the parameters of a pintle injector given by Ninishi, and the spray shape and atomization distribution after impingement of two water jets was simulated under the same injection condition. As shown in Figure 4, the comparison shows an acceptable agreement in the spray shape with a simulated spray angle of 142° similar to 145° in the experiment. Due to the low pressure drop in the reference, a thicker liquid-phase zone is aggregated along the edge of the impinged spray field, while the droplets size is much larger there. The simulative droplets size is close to the experimental droplets size, as shown in Figure 5. Therefore, the comparison indicates that this simulation method is suitable for pintle injector spray development analysis.

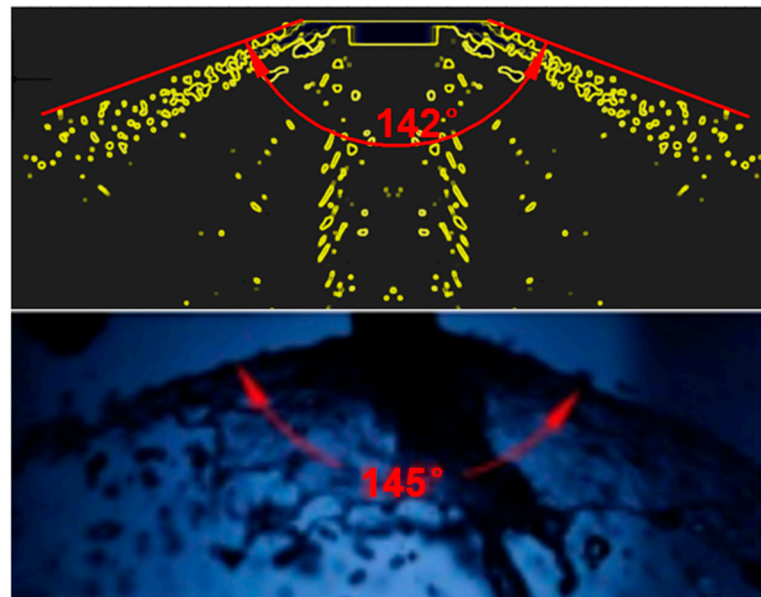


Figure 4. Comparison of spray simulation image and high-speed camera shot [30].

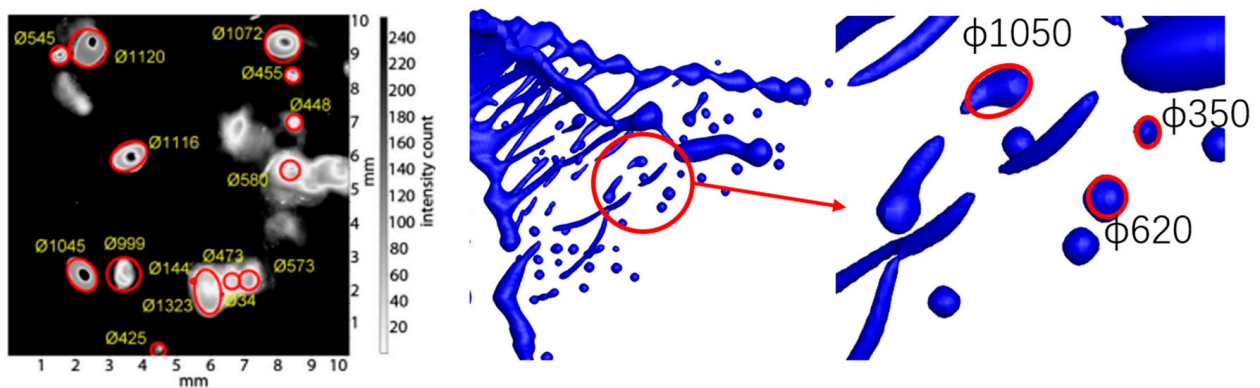


Figure 5. Comparison of simulative droplets size and experimental droplets size [30].

3. Results and Discussion

Under different conditions, the composite spray angle, atomization distribution, vortex location, total surface area ratio and mixing area are compared. The objective of optimization is to achieve a larger atomization angle and a more dispersed droplets distribution in terms of atomization visualization, and achieve a larger total surface area ratio and a larger mixed area in terms of atomization results. Those results benefit more rapid and uniform combustion, and at the same time the backflow effect is also expected to be better.

3.1. Effect of Flowrate

The advantage of a pintle injector is that when pressure potential energy is transformed into kinetic energy with high spray velocity, its energy loss is quite low due to a simple flow channel design. Meanwhile, there is an impingement effect during the process of sprayed kinetic energy to atomized surface energy, which enhances the growth of the disturbance short wave to accelerate the following atomization and mixing [31,32]. After the outer axial jet impinges on the inner radial jet, it forms a composite spray with a momentum angle. The magnitude of this angle mainly depends on the momentum ratio of the two jets. This angle has a decisive influence on the propellants distribution, which is a key to subsequent mixing, evaporation and combustion.

The spray atomization of a jet comes from liquid flow fluctuation instability and gas-liquid disturbance instability. The location and intensity of the vortex have an important influence on both instabilities. The vortex can strengthen the breakup and enhance spatial transport for better mixing.

Figure 6 shows visual differences between two pintle spray jets under different flowrates. The red is the MMH jet flow as the outer spray, while the blue is the NTO jet flow as the inner spray. The flowrate of two propellants is changed at the same time, so the momentum ratio of the radial jet and axial jet keeps unchanged. The baseline case is shown as Figure 6a with a pintle diameter of 10 mm and 48 narrow slots.

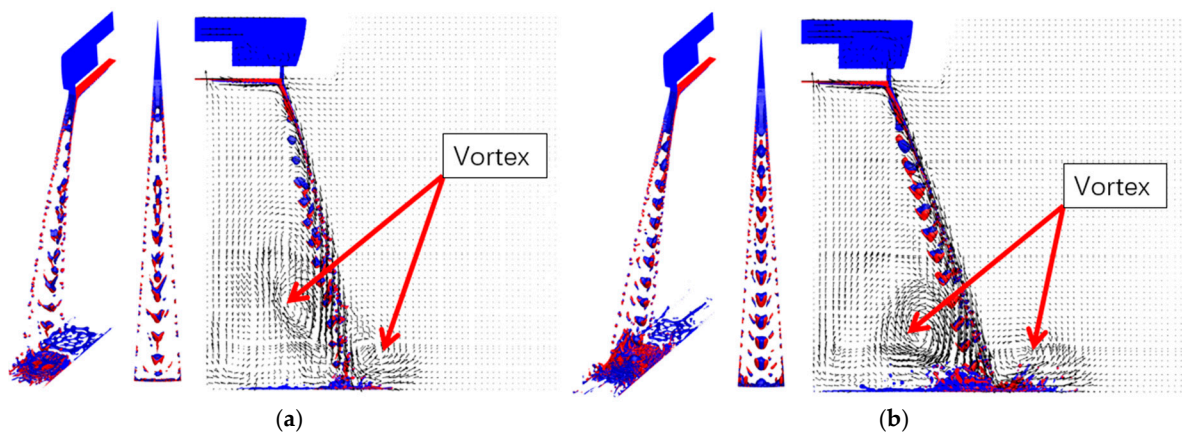


Figure 6. Comparison of spray visualization at 3 ms with pintle diameter 10 mm and 48 slots, (a) at standard flowrate, (b) at 30% larger flowrate.

Due to the combination effect of the slot and slit, a V-shaped jet flow is formed in the spray development. The slot jet generates the bottom of the V-shaped jet and the slit jet generates two edges of the V-shaped jet. More liquid ligaments and droplets are formed on the edge of the V-shaped jet in the breakup process. Since the radial NTO jet is much stronger than the axial MMH jet, the composite spray angle is quite large. The half composite spray angle is around 76° at standard flowrate and around 71° at 30% increased flowrate. With the increase in flowrate, the composite spray angle can slightly decrease, and a large backflow with vortexes is closer to the chamber wall, mainly caused by two reasons. The first reason is more violent spray impingement on the wall, and the second reason is that the higher flowrate easily carries the vortex to the downstream.

In the postprocessing, the atomization effect was characterized by calculating the total liquid surface area ratio over time, as shown in Figure 7. It shows the atomization quality and mixing effect by fitting the trend line at different time. As the flowrate increases, more propellant is sprayed out with more vortices, so R_{spray} and mixed area will also increase, as shown in Figure 7. In these comparative cases, the total surface area ratio increases by 30%, and the mixed area increases by around 45%, from 0.0035 mm² to 0.0051 mm². Due to the same injection pressure drop, injection velocity remains unchanged. Increasing the flowrate makes the liquid film thickened and difficult to breakup. However, the total atomization result is still strengthened under stronger impingement with larger vortices disturbance, which leads to the better atomization.

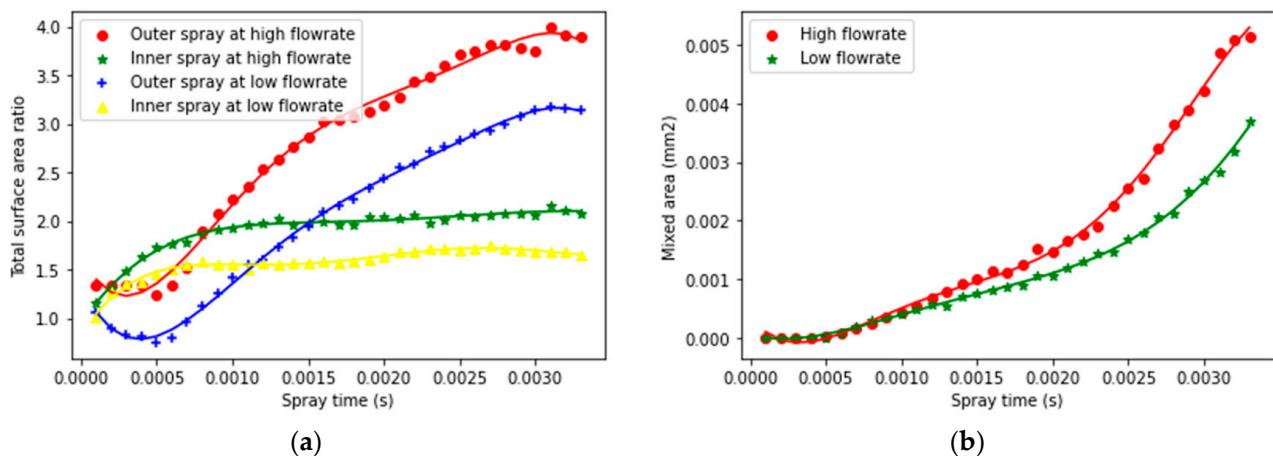


Figure 7. Comparison of (a) total surface area ratio and (b) mixed area of spray quantization with pintle diameter 10 mm and 48 slots at different flowrate over time.

3.2. Effect of Slots Number

In this subsection, the baseline case is the case of Figure 8a, which is the same as Figure 6a in the previous comparison. Under the condition of the same total flowrate, the flowrate of each single slot in 48 slots pintle must be smaller than that in 36 slots. Therefore, in terms of spray visual shape in Figure 8, its bottom of the V-shaped jet is weaker, and the size of the V-shaped jet bottom is slightly smaller. More liquid is distributed in the edge of the jet to form ligaments and droplets there. It causes that the slit jet to be more dominant compared with a single slot jet. Therefore, it can be clearly seen that the spatial distribution of the V-shaped jet is more concentrated, under the condition of pintle injector geometry with more slots. Its spray shape is close to the independent slit jet impingement without any slots. According to velocity distribution, as the number of slots decreases, the composite spray angle and vortex's location are almost unchanged, but the spatial distribution dispersion of the case with 36 slots increases relatively. It is concluded that the impinged spray caused by the radial annular slit is more concentrated, while the jet sprayed out of the radial slot makes its spray shape more dispersed. The combined effect of slit and slot depends on which one is more dominant.

Under the condition of different slot numbers, the overall atomization quality and mixing effect are almost similar, as shown in Figure 9. But the inner spray atomization of 36 slots is slightly stronger. As for the NTO jet, which is easily atomized, the effect of this improvement is limited. However, 36 slots can be seen as a more accepted optional scheme, because it is easier to manufacture with better dispersed spatial distribution.

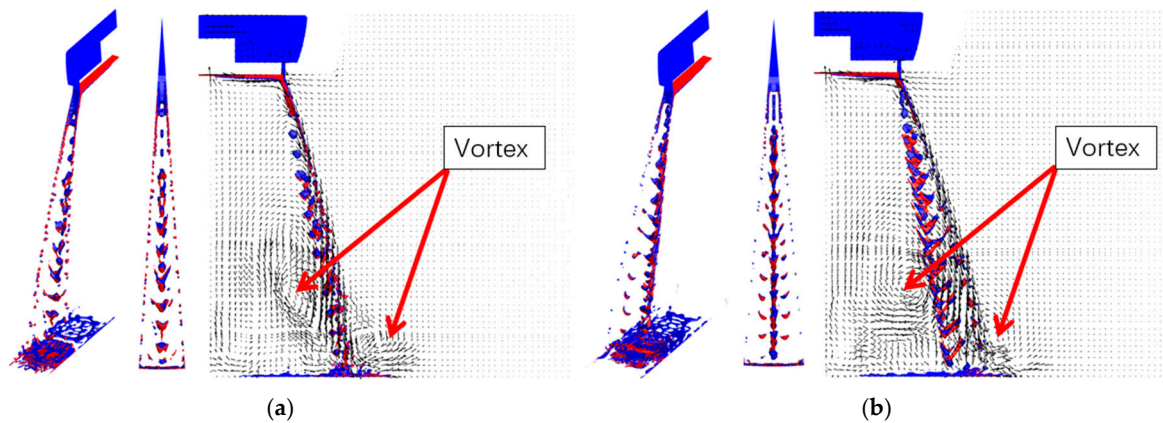


Figure 8. Comparison of spray visualization under the condition of standard flowrate at 3 ms with pintle diameter 10 mm, and (a) 48 slots and (b) 36 slots.

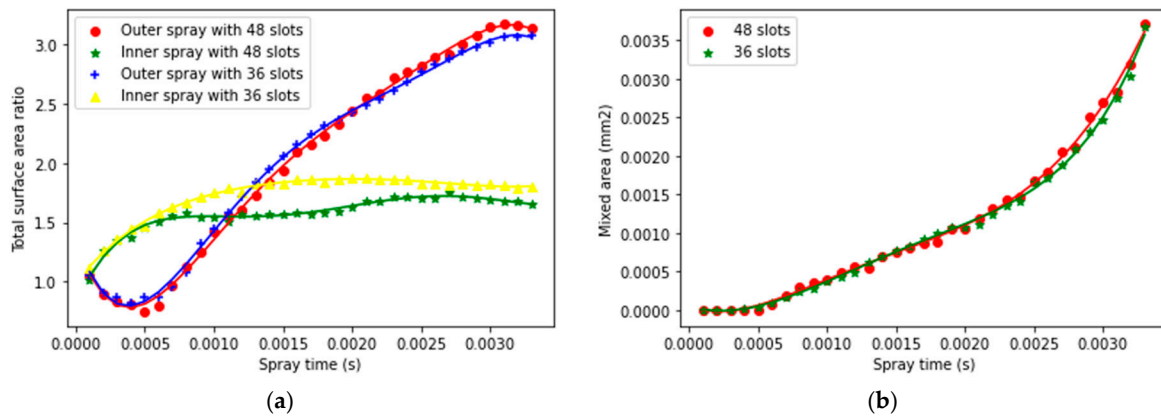


Figure 9. Comparison of (a) total surface area ratio and (b) mixed area of spray quantization at standard flowrate with pintle diameter 10 mm and different slots over time.

3.3. Effect of Pintle Diameter

In this subsection, the baseline case is changed to be the case of Figure 10a with a pintle diameter of 10 mm and 36 narrow slots, the same as Figure 8b. Figure 10 shows that the effect of increasing the pintle diameter is very obvious, under the condition of standard flowrate with 36 slots. When the pintle diameter was increased from 10 mm to 12 mm, the outer half angle of the composite spray increased from 80° to 83° , while the inner half angle of the composite spray decreased from 70° to 59° . That means the distribution of droplets changes greatly to be more dispersed. Therefore, although the proportional ratio of the slit jet and the slot jet is not adjusted, the V-shaped effect is more obvious and the spatial distribution is more ideal under the condition of a large pintle diameter. Thus, more liquid ligaments and droplets are generated along the V-shaped edge. Besides, there is a new vortex appearing close to the nozzle to enhance the aerodynamic interaction, under the condition of a large pintle diameter.

As shown in Figure 10, after increasing the pintle diameter, some changes were found in the location of the vortices. For the case with 12 mm pintle, the backflow on the jet panel side is obviously reduced by weakening the bottom of the V-shaped jet. But kinetic energy is concentrated in the front, while the vortex at the V-shaped edge is enhanced. Therefore, the vortex location overlaps the atomization area, which can more effectively benefit the secondary atomization.

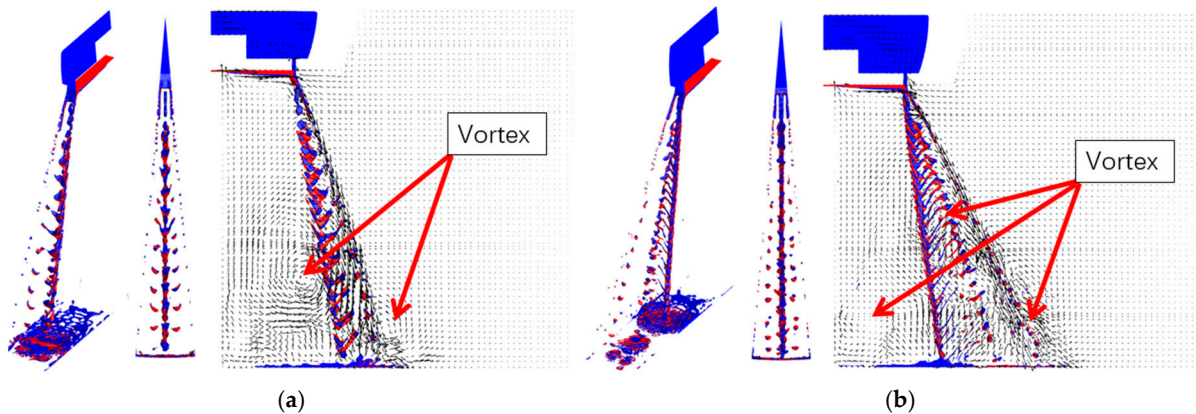


Figure 10. Comparison of spray visualization under the condition of standard flowrate at 3 ms with 36 slots, and (a) pintle diameter 10 mm and (b) pintle diameter 12 mm.

When the pintle diameter is increased, the atomization quality and the mixing effect are improved by about 10% under the same nozzle structure and pressure drop, as shown in Figure 11. The main reason is that increasing the diameter of the pintle makes the outer liquid film thinner and more unstable, under the condition of the same injection pressure drop and nozzle area. Although the effect of increasing the pintle diameter is completely positive, the manufacturable constraints of a too-thin gap should also be considered.

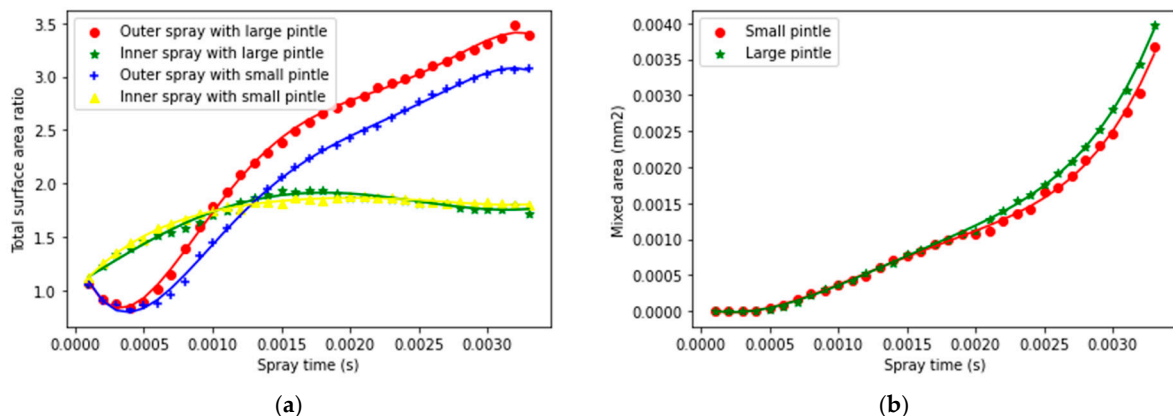


Figure 11. Comparison of (a) total surface area ratio and (b) mixed area of spray quantization at standard flowrate with 36 slots and different pintle diameter over time.

3.4. Effect of Slots Thickness

In this subsection, the baseline case is changed to be the case of Figure 12b with a pintle diameter of 12 mm and 36 narrow slots, which is the same as Figure 10b. When slot thickness is changed, the total area of the slot and slit remains unchanged with the same pressure drop. That means the slit area is increased while slot thickness is decreased. The change of slot thickness has little effect on the outer angle of the composite spray, as shown in Figure 13. However, under the same pressure, the thicker slot can take up more of the jet flow proportion, compared with the slit jet flow. It is the same to be said that the stronger slot jet leads to a smaller inner angle of the composite spray, resulting in a larger spatial distribution for droplets and ligaments. It is more conducive to the efficient use of the limited combustion chamber volume. Meanwhile, as the slot thickens, it can be seen that the location of vortices begins to significantly move towards the upstream. That means that gas–liquid disturbance appears earlier, which benefits atomization for better combustion.

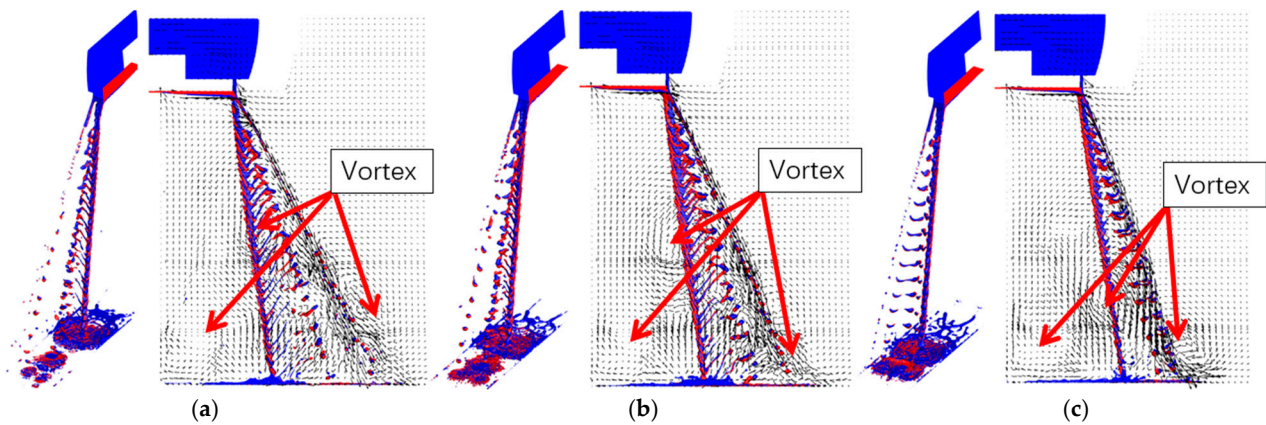


Figure 12. Comparison of spray visualization under the condition of standard flowrate at 3 ms with pintle diameter 12 mm and 36 (a) thick slots, (b) normal slots, (c) thin slots.

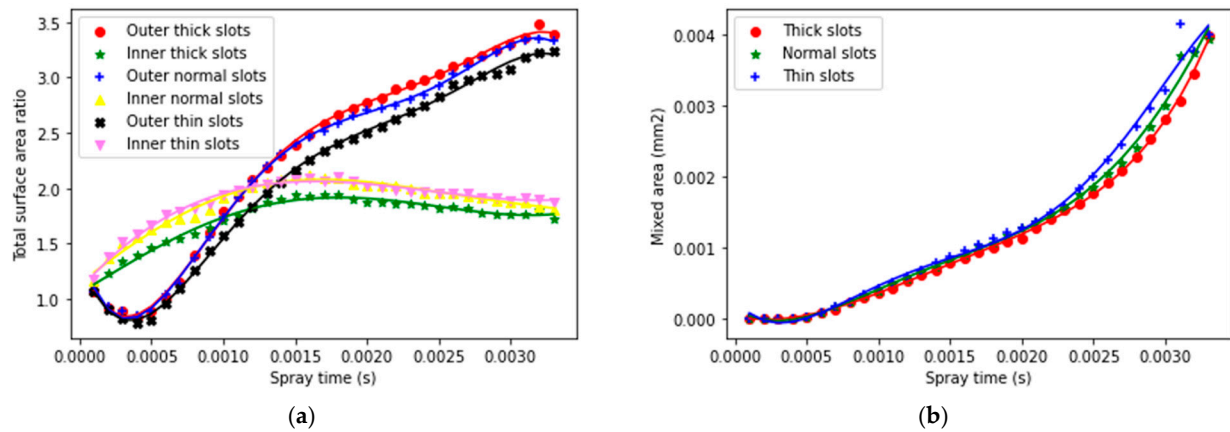


Figure 13. Comparison of (a) total surface area ratio and (b) mixed area of spray quantization at standard flowrate with pintle diameter 12 mm and 36 slots of different thicknesses over time.

As shown in Figure 13, the thin slot case leads to the worst inner spray atomization, while the normal slot case leads to the worst outer spray atomization. Therefore, the thick slot case can make the balance in the atomization quality of both inner and outer spray. The case with the thin slot is shown to obtain the largest mixed area, but the main mixed area of three cases just differentiates after 2.5 ms impingement on the chamber wall. Because the thin slot jet is more intensive, and the liquid mixing tends to be more concentrated after wall impingement, thus obtaining a larger mixing area. The geometry design needs to overall consider the spatial distribution, atomization and mixing quality. Therefore, when the atomization difference with different slots thickness is small, the spatial distribution is more important for optimization.

3.5. Effect of Slots Shape

In this subsection, the baseline case is the case of Figure 14a, which is still the same one in the previous two comparisons. As shown in Figure 14, the effect of slot shape is quite similar to slot thickness. The microarc slot can be seen as a thinner slot, resulting in a more concentrated jet flow. While for the semicircle slot jet, it is close to a normal slot jet both in the spray distribution and the vortex's location.

From the quantitative comparison in Figure 15, the case with a semicircle slot is an acceptable option in the geometry design. The total surface area ratio of a semicircle slot is the highest in the outer spray, and its atomization quality of the inner spray is not far away from the best case with a narrow slot. Meanwhile, the result of its mixing effect is better than

the regular narrow slot case. Because, for a semicircle slot, there are three vortices close to the nozzle to improve the atomization distribution. In addition, compared with the narrow slot case, the semicircle slot is easier to manufacture with precise dimensional control.

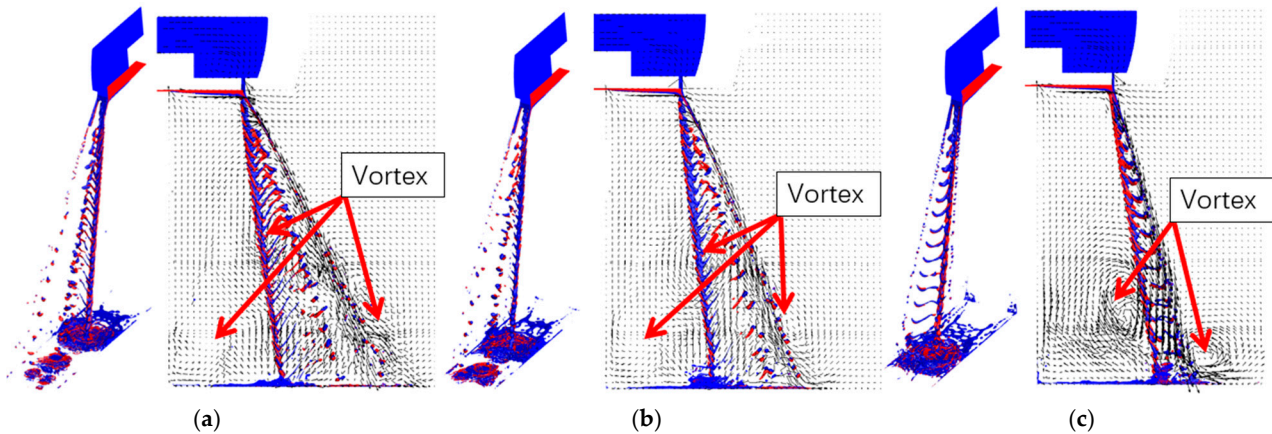


Figure 14. Comparison of spray visualization under the condition of standard flowrate at 3 ms with pintle diameter 12 mm and 36 (a) narrow slots, (b) semicircle slots, (c) microarc slots.

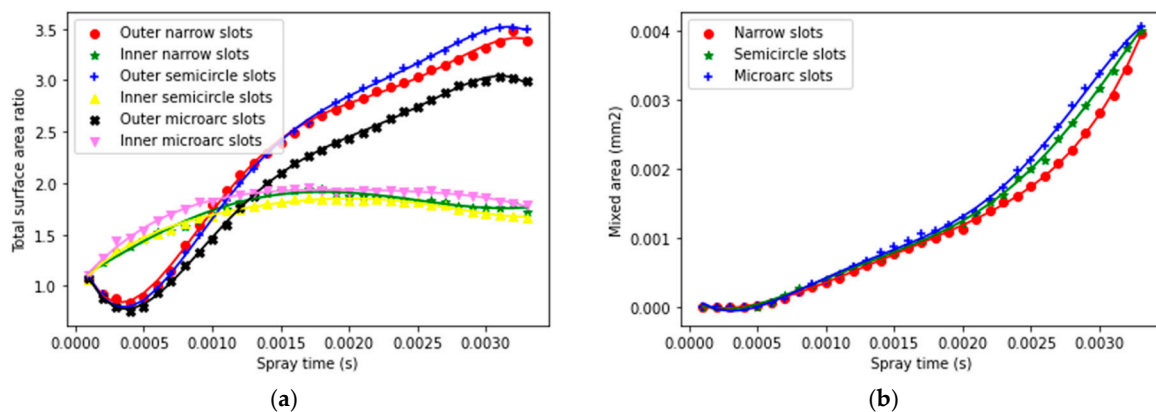


Figure 15. Comparison of (a) total surface area ratio and (b) mixed area of spray quantization at standard flowrate with pintle diameter 12 mm and 36 slots of different shape over time.

4. Conclusions

The impinging spray development of a pintle injector was numerically investigated, motivated to improve the performance of a bipropellant engine with high efficiency. In particular, the research focuses on the effects of geometry design on slit/slot radial jet impinging on the annular axial jet. The composite spray angle, atomization quality and mixing effect are compared in visualization and quantification.

The combination effect of slit and slot generates a V-shaped jet flow after impingement. More ligaments and droplets are generated along the V-shaped edge. Increasing the flowrate can enhance the impinging effect, and increasing the pintle diameter can reduce the thickness of the annular liquid film. Increasing the flowrate by 30% can cause the total surface area ratio to be increased by around 30%, and the mixed area to be increased by around 45%. Increasing the pintle diameter can lead to better atomization quality and mixing effect by around 10% with dispersed atomization. The difference caused by the slot number, slot thickness and slot shape is more important in the influence of spray spatial distribution. The key lies in the jet flow proportion of slot and slit. When the slit jet is dominant, the composite spray is more concentrated. And when the slot jet is stronger, the composite spray is more dispersed, which is more conducive to the subsequent improvement of combustion efficiency in limited space. However, continuously increasing

the flow proportion of the slot jet might lead to a gradual decline in the mixing effect, so a balance should be optimized in the geometry design.

In future work, pintle injector element experiments with machine learning modeling will be conducted. In this way, the Reynolds stress is modified in the original governing equation to strengthen the description of the strong nonlinear process of jet impingement.

Author Contributions: Conceptualization, K.C., Z.Z. and F.W.; methodology, X.W. and Y.Y.; software, Z.Z.; validation, K.C.; formal analysis, Y.H.; investigation, K.C. and Z.Z.; resources, K.C. and H.L.; data curation, F.W. and Z.F.; writing—original draft preparation, K.C.; writing—review and editing, Z.Z.; visualization, Y.H.; supervision, Z.Z., Y.Y. and H.L.; project administration, X.M. and Z.Y.; funding acquisition, H.L. All authors have read and agreed to the published version of the manuscript.

Funding: This research was supported by the National Key R&D Program of China (2022YFC2001002).

Institutional Review Board Statement: Not applicable.

Informed Consent Statement: Not applicable.

Data Availability Statement: Not applicable.

Conflicts of Interest: The authors declare no conflict of interest.

References

1. Wang, K.; Lei, F.P.; Yang, A.L.; Yang, B.E.; Zhou, L.X. Numerical simulation of spray and mixing process of impingement between sheet and jet in pintle injector element. *Acta Aeronaut. Astronaut. Sin.* **2020**, *41*, 123802.
2. Heister, S.D. *Handbook of Atomization and Sprays: Theory and Applications*; Springer Science + Business Media: New York, NY, USA, 2011; pp. 647–655.
3. Dressler, G.A. Summary of deep throttling rocket engines with emphasis on Apollo LMDE. In Proceedings of the 42nd AIAA/ASME/SAE/ASEE Joint Propulsion Conference & Exhibit Sacramento, Sacramento, CA, USA, 9–12 July 2006; pp. 2006–5220.
4. Lei, J.P.; Lan, X.H.; Zhang, R.J.; Chen, W. Development of 7500 N variable thrust engine for Chang'e-3 probe. *Sci. Sin. Technol.* **2014**, *44*, 569–575.
5. Sun, Z.Z.; Jia, Y.; Zhang, H. Technological advancements and promotion roles of Chang'e-3 lunar probe mission. *Sci. China Technol. Sci.* **2013**, *56*, 2702. [[CrossRef](#)]
6. Li, J.; Chang, K.Y.; Chen, Z. Design and Experimental Study of Liquid Oxygen/Methane Thrust Chamber for Pintle Injector. *J. Propuls. Technol.* **2022**, *43*, 210570.
7. An, P.; Yao, S.Q.; Wang, J.L.; Zhou, W.L. Characteristics and design of pintle injector. *Missiles Space Veh.* **2016**, *345*, 50–54.
8. Dressler, G.A.; Bauer, J.M. TRW pintle engine heritage and performance characteristics. In Proceedings of the 36th AIAA/ASME/SAE/ASEE Joint Propulsion Conference and Exhibit Huntsville, Huntsville, AL, 16–19 July 2000; pp. 2000–3871.
9. Son, M.; Yu, K.; Koo, J.; Kwon, O.C.; Kim, J.S. Effects of momentum ratio and Weber number on spray half angles of liquid controlled pintle injector. *J. Therm. Sci.* **2015**, *24*, 37–43. [[CrossRef](#)]
10. Son, M.; Yu, K.; Radhakrishnan, K.; Shin, B.; Koo, J. Verification on spray simulation of a pintle injector for liquid rocket engine. *J. Therm. Sci.* **2016**, *25*, 90–96. [[CrossRef](#)]
11. Son, M.; Radhakrishnan, K.; Koo, J.; Kwon, O.C.; Kim, H.D. Design procedure of a movable pintle injector for liquid rocket engines. *J. Propuls. Power* **2017**, *33*, 858–869. [[CrossRef](#)]
12. Rezende, R.N.; Pimenta, A.; Perez, V.C. Experiments with pintle injector design and development. In Proceedings of the 51th AIAA/SAE/ASEE Joint Propulsion Conference, Orlando, FL, USA, 27–29 June 2015.
13. Fang, X.; Shen, C. Study on atomization and combustion characteristics of LOX/methane pintle injectors. *Acta Astronaut.* **2017**, *136*, 369–379. [[CrossRef](#)]
14. Ryu, H.; Yu, I.; Kim, T.; Ko, Y.; Kim, S.; Kim, H. Combustion performance of the canted slit type pintle injector rocket engine by blockage factor. In Proceedings of the Korean Society of Propulsion Engineers Conference, Jeju, Republic of Korea, 25–27 May 2016.
15. Yu, I.; Kim, S.; Ko, Y.; Kim, S.; Lee, J.; Kim, H. Combustion performance of a pintle injector rocket engine with canted slit shape by characteristic length and total momentum ratio. *J. Korean Soc. Propuls. Eng.* **2017**, *21*, 36–43. [[CrossRef](#)]
16. Kim, S.; Kim, W.; Kim, T.; Ko, Y.; Kim, S.; Kim, H. Analysis on combustion phenomena by spray pattern of canted slit type pintle injector. In Proceedings of the Korean Society of Propulsion Engineers Conference, Jeju, Republic of Korea, 8–10 June 2016.
17. Zhou, R.; Shen, C. Experimental study on the spray characteristics of a pintle injector element. *Acta Astronaut.* **2022**, *194*, 255–262. [[CrossRef](#)]
18. Chen, H.; Li, Q.; Cheng, P. Experimental research on the spray characteristics of pintle injector. *Acta Astronaut.* **2019**, *162*, 424–435. [[CrossRef](#)]
19. Cheng, P.; Li, Q.; Chen, H. Flow characteristics of a pintle injector element. *Acta Astronaut.* **2019**, *154*, 61–66. [[CrossRef](#)]

20. Xu, W.; Gao, X.N.; Hu, B.L.; Yang, J.W.; Yang, B.; Ying, W. Numerical simulation of primary breakup and secondary atomization for centrifugal nozzle. *J. Rocket Propuls.* **2022**, *48*, 13–20.
21. Nazeer, Y.H.; Ehmann, M.; Sami, M.; Gavaises, M. Atomization Mechanism of Internally Mixing Twin-Fluid Y-Jet Atomizer. *J. Energy Eng.* **2021**, *147*, 04020075. [[CrossRef](#)]
22. Li, H.; Feng, J.; Cao, X.; Zhang, Z.; Liang, H.; Yu, Y. Simulation Study of the Swirl Spray Atomization of a Bipropellant Thruster under Low Temperature Conditions. *Energies* **2022**, *15*, 8852. [[CrossRef](#)]
23. Wang, L.; Fang, B.; Wang, G.C. Process of Pressure Swirl Nozzle Atomization Based on Large Eddy Simulation. *J. Propuls. Technol.* **2021**, *42*, 1855–1864.
24. Yu, L.; Zhou, H.M. LES/VOF Numerical Simulation of Flow in Centrifugal Nozzle. *J. Nav. Aeronaut. Astronaut. Univ.* **2017**, *32*, 154–160.
25. Clark, R.A.; Ferziger, J.H.; Reynolds, W.C. Evaluation of subgrid-scale models using an accurately simulated turbulent flow. *J. Fluid Mech.* **1979**, *91*, 1–16. [[CrossRef](#)]
26. Menon, S. Subgrid combustion modelling for large-eddy simulations. *Int. J. Thruster Res.* **2000**, *1*, 209–227. [[CrossRef](#)]
27. Ninish, S.; Vaidyanathan, A.; Nandakumar, K. Spray characteristics of liquid-liquid Pintle injector. *Exp. Therm. Fluid Sci.* **2018**, *97*, 324–340. [[CrossRef](#)]
28. Zhang, Z.; Shin, D. Effect of ambient pressure oscillation on the primary breakup of cylindrical liquid jet spray. *Int. J. Spray Combust. Dyn.* **2020**, *12*, 1756827720935553. [[CrossRef](#)]
29. Luo, F.Q.; Deng, R.; Wang, Y.Q.; Yan, Z.P.; Wu, T.C. Research on the Calculation Strategy of Adaptive Mesh Refinement Based on OpenFOAM. *Shipbuild China* **2020**, *61*, 169–178.
30. Zhang, Z.; Yu, Y.; Cao, J. Effect of Upstream Valve Opening Process on Dynamic Spray Atomization. *Micromachines* **2022**, *13*, 527. [[CrossRef](#)]
31. Dombrowski, N.; Hooper, P.C. The effect of ambient density on drop formation in sprays. *Chem. Eng. Sci.* **1962**, *17*, 291–305. [[CrossRef](#)]
32. Dombrowski, N.; Johns, W.R. The aerodynamic instability and disintegration of viscous liquid sheets. *Chem. Eng. Sci.* **1963**, *18*, 203–214. [[CrossRef](#)]

Disclaimer/Publisher’s Note: The statements, opinions and data contained in all publications are solely those of the individual author(s) and contributor(s) and not of MDPI and/or the editor(s). MDPI and/or the editor(s) disclaim responsibility for any injury to people or property resulting from any ideas, methods, instructions or products referred to in the content.